ELSEVIER

Journal of Chromatography A, 964 (2002) 77–89

JOURNAL OF CHROMATOGRAPHY A

www.elsevier.com/locate/chroma

Fluidisation and dispersion behaviour of small high density pellicular expanded bed adsorbents

Irini Theodossiou, H. David Elsner, Owen R.T. Thomas, Timothy J. Hobley*

Center for Process Biotechnology, BioCentrum-DTU, Technical University of Denmark, Building 223, Søltofts Plads, DK-2800 Lyngby, Denmark

Received 18 September 2001; received in revised form 4 April 2002; accepted 8 May 2002

Abstract

The fluidisation and dispersion properties of various agarose-based expanded bed matrices—small high density stainless steel cored prototypes and standard commercial types—were studied in 1-cm diameter expanded bed contactors in which fluid entering the column base is locally stirred. In all cases, fluidisation behaviour was poorly predicted from the Richardson–Zaki correlation, with experimentally determined values of the expansion index being considerably higher than the theoretical values. The reasons for these discrepancies are discussed in detail and the validity of applying this widely used correlation for characterisation of expanded bed systems is questioned. Residence time distribution studies using acetone tracers, demonstrated that in comparison to existing commercial supports, the small pellicular prototype materials generally possessed far superior hydrodynamic properties, which augurs well for their future employment in expanded bed chromatographic separations.

Keywords: Dispersion; Expanded bed adsorption; Fluidized bed chromatography; Adsorbents; Liquid–solid fluidization

1. Introduction

Conventional packed bed chromatography supports were the starting point for development of expanded bed adsorption (EBA) adsorbents, but these exhibited poor fluidisation properties [1]. Fluidisation was improved by raising the terminal settling velocity (U_t) of the support through an increase in the particle diameter to 100–300 μm and density to ~1200 kg m^{-3} [2] according to the well-known Stokes equation (Eq. (1)):

$$U_t = \frac{(\rho_p - \rho_l) \cdot d_p^2 \cdot g}{18\eta} \quad (1)$$

where ρ_p is the density of the support, ρ_l is the density of the liquid, d_p is the support diameter, g is acceleration due to gravity and η is the solution viscosity.

A distribution of support diameters in the range of 100–300 μm results in formation of a classified fluidised bed, with the largest particles at the bottom of the column and the smallest at the top [3,4]. In this way axial mixing of adsorbent is reduced and ''product''-loaded matrix at the bottom does not mix with unloaded support higher up, which would otherwise result in early product breakthrough during feedstock application. A size ratio of the largest to

*Corresponding author. Tel.: +45-4525-2706; fax: +45-4588-4148.

E-mail address: th@biocentrum.dtu.dk (T.J. Hobley).

0021-9673/02/$ – see front matter
PII: S0021-9673(02)00590-3

smallest particles (of similar density) of more than 2.2 [3], or a ratio of minimum fluidising velocities greater than ~2 [4] is required for a classified fluidised bed to form. In support of this Karau et al. [5] showed that for EBA a wide support size distribution (120–300 μm) results in less liquid phase dispersion than a narrow distribution (120–160 or 250–300 μm).

Thömmes [6] reviewed the hydrodynamic aspects of expanded bed adsorption and concluded that out of the five main system parameters considered, no single one controlled the efficiency of protein adsorption, but that mass transport within the support plays a dominant role. The latter conclusion is consistent with Draeger and Chase's [1] earlier finding that in EBA the rate of protein binding to a support is pore diffusion and film mass transfer controlled. Mass transport is influenced mainly by the effective diffusion coefficient and particle diameter [6]. Thömmes [6] proposed a number of design criteria that should lead to improved separation performance in EBA. These included a reduction in particle size to reduce the length for protein diffusion, in conjunction with an increase in density to allow the use of high flow-rates (reducing the mass transfer limit within the liquid film surrounding the support) whilst controlling bed voidage, and a gradient in support size and/or density to limit axial dispersion. Support for this was found by Karau et al. [5] who showed that reducing the diameter of a DEAE-linked adsorbent did lead to improved breakthrough capacities for BSA and that mass transfer within the liquid film surrounding the support then became one of the limiting factors controlling protein adsorption. In addition to the mass transport benefits of small supports, the dispersion coefficient in fluidised beds of a given voidage is generally lower for smaller particles [7,8], since a lower liquid velocity is required than for larger faster settling supports, which leads to less turbulence and mixing [7].

Recently, new types of expanded bed adsorbent have been reported [9–14] that may fulfill many of the requirements discussed above. The prototype supports designed and employed by Theodossiou and co-workers [9–12] were small (20–40 μm in diameter) stainless steel–agarose composites of high density (~3700 kg m^{-3}). The supports were variously derivatised with anion exchangers or triple helix affinity ligands [10] and were designed specifically for the recovery of nanoparticulate molecules [15], such as plasmid DNA, from crude feedstocks. Binding capacities were significantly increased compared to conventional EBA supports, primarily as a result of the enhanced external surface area for capture. The fluidisation behaviour and hydrodynamic properties were not examined in detail, but it was reported that the prototypes expanded slightly more than conventional 100–300 μm EBA supports [11]. The EBA supports described by Pålsson et al. [13,14] were also crosslinked agarose/stainless steel composites containing one or more dense cores, but were of larger size than those studied by Theodossiou et al. [11], although similar density (d_p = 32–75 μm or 75–180 μm; ρ_p = 4400 or 3300 kg m^{-3}). A brief hydrodynamic evaluation [13] of axial liquid mixing during fluidisation of the supports was compared in a later report [14] to theoretically expected values and to results by Thömmes et al. [16], however fluidisation behaviour was not studied in depth.

The Richardson–Zaki correlation [17] describes the effect of suspended particle concentration (i.e., voidage) on the rate of settling and allows prediction of the liquid velocity required to produce a given degree of bed expansion during fluidisation. The correlation is confined to uniformly sized, non-porous, spherical particles greater than 100 μm in diameter with the same density. The Richardson–Zaki correlation is, additionally, not suitable for modeling particle mixing [3]. This said, it is nevertheless commonly employed to predict and model the expansion behaviour of EBA columns used in bioseparations (see, for example, Refs. [1,2,6,8]) even though the model often does not agree with the experimental results.

In this paper we describe the fluidisation and dispersion properties of the small, high density pellicular expanded bed matrices introduced by us previously [9–12], in a 1 cm diameter column in which localised stirring at the base of the contactor is employed to distribute the incoming fluid [18]. Experimentally determined data from bed expansion studies were used to test the applicability of the widely used Richardson–Zaki correlation [17] and residence time distribution experiments employing acetone tracer were subsequently conducted in order

to assess the possible benefits of the new materials over currently existing ones for expanded bed adsorptive separations.

2. Materials and methods

2.1. Supports

Prototype supports with mean diameters between 32 and 38 μm and particle densities of 3960–4780 kg m^{-3} were composed of spherical stainless steel cores encased in a thin layer of cross-linked 6% agarose. These materials were variously derivatised with the following anion-exchange groups: diethylaminoethyl (DEAE); dextran tentacles functionalised with DEAE; or high-molecular mass (50 kDa) polyethyleneimine (PEI), and were received as gifts from UpFront Chromatography (Copenhagen, Denmark). Commercial DEAE and PEI-linked UFC EBA adsorbents were also received from UpFront Chromatography and were composed of one or more glass cores incorporated within crosslinked 6% agarose beads. Diameters were in the range of ~100–300 μm and densities were 1380 and 1520 kg m^{-3} for the DEAE and PEI functionalised materials, respectively. The STREAMLINE™ anion exchange (DEAE and QXL) adsorbents (d_p = 70–300 μm, ρ_d = 1150 kg m^{-3}) employed in this study consisted of crosslinked 6% agarose beads impregnated with quartz grains and were supplied by Amersham–Biosciences (Uppsala, Sweden).

2.2. Operation of the EBA column

A FastLine™ 10 column (UpFront Chromatography) with a 1 cm internal diameter and 40 cm height, employing localised stirring (LS) for fluid distribution, was used. The column was placed on a Heidolph MR2000 stirrer (Heidolph, Germany) rotating at 750 rpm, which facilitated fluid distribution using a magnetic stirring bar (~0.5 cm long) located immediately above a liquid inlet hole, ~1–2 mm in diameter in the column base. This system is particularly suited to use with small supports (i.e., <60 μm diameter) since other EBA columns typically employ plates and meshes with ~60 μm holes for fluid distribution. In all experiments, the mixing zone was less than 2.5 cm high; however, the column construction prohibited measurement of mixing zones below 2.5 cm. Prior to support loading, the column was partially filled with fluid using a Microperpex 2232 peristaltic pump (LKB, Bromma, Sweden). The settled bed height (H_o) was determined after the bed was fluidised and allowed to settle. During bed expansion studies, water was applied to the matrix under test at the desired rate and the bed was allowed to stabilise for at least 0.25 h before measuring the expanded bed height (H). The residence time distribution of a 0.45% (v/v) solution of acetone in water was determined using the negative step input method [2,19,20] and the concentration of acetone in the column effluent was monitored by measuring the adsorbance at 280 nm using an on-line UV-1 detector (Amersham–Biosciences). The resulting F-curve was then differentiated to yield the corresponding C-pulse curve. The first and second moments of the distribution were used to give the mean and variance of the tracer, from which the plate number and vessel dispersion number were determined according to the tanks-in-series and dispersion models.

2.3. Analysis

Support size distributions were determined by measuring the diameter of between 260 and 460 adsorbent particles with the aid of a Nikon Optiphot 2 microscope (Nikon, Melville, NY, USA) fitted with a Kappa CF-8/1 FMC monochrome video camera (Kappa Opto-electronics, Gleichen, Germany) in conjunction with Image-Pro® Plus software (version 4.1 for Windows™; Media Cybernetics, Silver Spring, MD, USA). The bulk densities of the supports were calculated by weighing a known settled volume (0.5 or 1 ml) of each matrix and the particle densities were then estimated by assuming, from the random bed theory, that the voidage of a settled bed is 0.418 (see Ref. [21] and Refs. therein).

3. Theory

3.1. Fluidisation

The application of the Richardson–Zaki correla-

tion to predictions of EBA bed expansion is made assuming that all the supports are of the same average size. Following the approach of Richardson and Zaki [17], U_t can be determined from Eq. (1) for the case where the particle Reynolds number $Re_p < 0.2$ [2]. The particle Reynolds number at the terminal settling velocity (Re_t) of the support can then be calculated from Eq. (2) and used to decide which of Eqs. (3), (4) or (5) should be applied in order to determine the value of the expansion index n from the ratio of d_p and column diameter (d_c).

$$Re_t = \frac{U_t \cdot d_p \cdot \rho_l}{\eta} \quad (2)$$

$$n = 4.65 + 19.5 d_p/d_c \quad Re_t < 0.2 \quad (3)$$

$$n = (4.35 + 17.5 d_p/d_c) Re_t^{-0.03} \quad 0.2 < Re_t < 1 \quad (4)$$

$$n = (4.45 + 18 d_p/d_c) Re_t^{-0.1} \quad 1 < Re_t < 500 \quad (5)$$

EBA supports are generally assumed to be spherical and in the majority of cases to have a diameter much less than that of the column ($d_p/d_c < 0.01$) where wall effects (i.e., a velocity gradient created by drag exerted by the walls) are not significant [17,21] and to have values of $Re_t < 0.2$ where laminar liquid flow around the particle occurs. Thus n is essentially independent of d_p/d_c and a value of n close to 4.65 is often predicted. The n-index can be substituted into Eq. (6) to determine the relationship between bed voidage (ε), the interstitial fluid velocity (U_i) and superficial fluidising velocity (U). The fluidised bed height can then be predicted from Eq. (7) assuming a settled bed voidage (ε_o) of 0.418 [21].

$$U = U_t \cdot \varepsilon^n \quad (6)$$

$$\frac{H}{H_o} = \frac{(1 - \varepsilon_o)}{(1 - \varepsilon)} \quad (7)$$

To test the validity of the Richardson–Zaki correlation, Eqs. (6) and (7) can be fitted to experimental data. Furthermore, U_t and n can be determined experimentally from bed expansion data by finding the slope (n) and y-intercept (U_t) of a $\log U$ versus $\log \varepsilon$ plot [1,8,17]. Under a specific set of conditions for a given support, n is independent of voidage.

In a bed composed of supports with a range of sizes and terminal settling velocities, there is a gradual transition from settled to fluidised bed. The range of flow-rates that can be used in EBA must be between the minimum fluidisation velocity (U_{mf}) of the bed (i.e., of the largest supports) and the U_t of the smallest supports. The U_{mf} for beds of particles has been reviewed by many authors (see, for example, Refs. [4,22,23]) and the correlation described in Eq. (8) for the Reynolds number at minimum fluidisation (Re_{mf}) can be derived assuming $\varepsilon_o = 0.418$. The Galileo number (Ga) is proportional to the terminal Reynolds particle number [4] and can be determined from Eq. (9).

$$Re_{mf,\varepsilon=0.418} = 24.9 \cdot \left(\sqrt{1 + 6.71 \times 10^{-5} \cdot Ga} - 1\right) \quad (8)$$

$$Ga = 18 \cdot Re_t \quad (9)$$

3.2. Liquid mixing and dispersion in fluidised beds

In a classified fluidised bed, mixing of ''loaded'' adsorbent particles with ''unloaded'' ones is restricted. However, chromatographic performance may also be affected by axial mixing of the liquid. Axial mixing in EBA columns is often characterised using the tanks-in-series or dispersion models to fit experimentally obtained data from the residence time distribution (RTD) of a tracer. Following the stepwise or pulse addition of tracer to the fluidised bed, the concentration profile at the outlet is measured.

The dispersion model uses a single parameter to describe mixing, which is termed the vessel dispersion number, $D_{axl}/(U_i \cdot H)$; where D_{axl} is the axial dispersion coefficient and describes the degree of mixing in the direction of flow through the column, U_i is the interstitial fluid velocity ($U_i = U/\varepsilon$) and H is the height of the expanded bed. The vessel dispersion number relates convective transport of liquid to dispersion and is used to describe the influence of axial mixing on the performance of the whole fluidised bed set-up [6,20,21]. Using a negative step input of tracer, a short-cut method can be used with the dispersion model when the vessel dispersion number is low (i.e., $D_{axl}/(U_i \cdot H) < \sim 0.01$). At such small extents of dispersion, the

boundary conditions (i.e., open or closed) imposed on the vessel have little impact on the shape of the tracer curve and a Gaussian approximation for the RTD can be assumed [20,24]. The dimensionless variance (σ_θ^2) can be calculated from Eq. (10) and used in Eq. (11) to determine the vessel dispersion number. If there is a large deviation from plug flow ($D_{axl}/(U_i \cdot H) > \sim 0.01$), i.e., the tracer response is broad and spreads as it slowly passes the measurement point giving an asymmetric response [20], the assumptions made in the use of the short-cut method are no longer valid. Closed boundary conditions must therefore be used (i.e., it is assumed that the flow pattern at the inlet and outlet is different to that within the EBA column) and Eq. (12) chosen to determine the vessel dispersion number. Use of Eq. (12) requires that the so-called F-curve resulting from a step change in tracer concentration be differentiated to yield the corresponding C-pulse curve [20]. The C-pulse curve is then normalised to unity and the first and second moments determined to give the mean residence time (t_m) and the variance (σ^2), respectively [20,25] which can be used to give σ_θ^2 according to Eq. (10) and which can in turn be used in Eq. (12) to yield the vessel dispersion number.

$$\sigma_\theta^2 = \frac{\sigma^2}{t_m^2} \tag{10}$$

$$\sigma_\theta^2 = 2 \cdot \left(\frac{D_{axl}}{U_i \cdot H} \right) \tag{11}$$

$$\sigma_\theta^2 = 2 \cdot \left(\frac{D_{axl}}{U_i \cdot H} \right) - 2 \cdot \left(\frac{D_{axl}}{U_i \cdot H} \right)^2 \cdot \left(1 - \varepsilon^{-\left(\frac{U_i \cdot H}{D_{axl}} \right)} \right) \tag{12}$$

The tanks-in-series model also uses one parameter, the number of theoretical plates, N, to describe mixing. From a negative step input of tracer, t_m and the standard deviation (σ) are determined [2,19,20], which in turn can be used to calculate N, from Eq. (13). The height equivalent to a theoretical plate, HETP can subsequently be determined (HETP = H/N). As the values of N increase, the RTD curves become increasingly symmetrical and a short cut method can also be used with the tanks-in-series model, where 2σ is determined from the 16th and 84th percentile of the F-curve [24]. Under these conditions the tanks-in-series and dispersion models can be coupled through Eqs. (10), (11) and (13) [20,24,26].

$$N = \frac{t_m^2}{\sigma^2} \tag{13}$$

The use of pore-penetrating tracers such as acetone can be expected to cause lengthening of the tail of the RTD curve [24], leading to band broadening. Thus a higher residence time and greater variance due to the diffusion of the tracer in the support pores [14] can be expected when compared to non-penetrating tracers. However, by using a pellicular support having a very thin agarose layer, and a small rapidly diffusing tracer such as acetone, the effect of pore diffusion on the values of D_{axl} and N determined in the bulk fluid can be reduced. In contrast, the dominance of the diffusive effects of larger tracers such as proteins, would be expected to lead to a significant increase in the value found for HETP as U is raised [14].

4. Results and discussion

4.1. Support properties

The physical properties of the supports were determined prior to examining their fluidisation behaviour. The measured size distributions show that the mean diameters of the prototypes lay between 32.3 and 37.3 μm (Table 1), whereas those for the commercial materials were ~143 and 175 μm for STREAMLINE and UFC adsorbents, respectively. Representative size distribution profiles are shown in Fig. 1 and were, in general, asymmetric bell shapes except for support p-4 (Fig. 1b). Some prototype particles were not spherical and between 8 and 46% of the populations had more than one core, resulting in an ovoid shape and a variable ratio of core to agarose volume (Fig. 2a). In addition, supports containing a single stainless steel bead, also possessed an agarose layer depth which varied from particle to particle (Fig. 2b–d). By measuring the percentage of the support volume occupied by the core and by assuming densities of 1020 and 7800 kg

Table 1
Fluidisation properties of prototype and commercial supports in a 1-cm diameter Fastline™ column

Support code	Support and batch number[a]	Support diameter distribution and (μm)	mean	Support density (kg m^{-3})	Stokes[b] U_t range and (cm h^{-1})	mean	Richardson–Zaki[c]			Experimental[d]		
							n	Re_t	Re_{mf}	n	U_t (cm h^{-1})	Re_t
p-1	p-no ligand 61374J	28–44	37.3	3960	455–1123	807	4.72	0.083	0.001	5.62	784	0.080
p-2	p-DEAE 61581J	26–46	34.1	4330	441–1380	759	4.72	0.072	0.001	5.81	760	0.071
p-3	p-dexDEAE 61635J	26–42	32.3	4780	501–1306	773	4.71	0.069	0.001	5.66	832	0.073
p-4	p-PEI 61474J	18–50	34.8	4250	206–1592	771	4.72	0.074	0.001	5.02	685	0.066
U-1	UFC-DEAE DEFD002	100–300[e]	200[e]	1380	748–6728	2990	4.76	1.66	0.025	6.12	4594	2.4
U-2	UFC-PEI IOFD003	110–300	174.6	1520	1236–9196	3115	4.77	1.5	0.023	6.16	5669	2.6
S-1	STREAMLINE DEAE 277891	70–300	142.7	1150	145–2675	605	5.11	0.24	0.004	6.10	1221	0.48
S-2	STREAMLINE QXL 277048	70–260	142.5	1150	145–2009	604	5.11	0.24	0.004	6.55	2005	0.76

[a] p- denotes prototype support, other supports are commercially available.
[b] Calculated from Eq. (1) assuming $\eta = 0.001002$ kg m^{-1} s^{-1} and $\rho_l = 998.2$ kg m^{-3} for water at room temperature.
[c] Using Eqs. (1), (2–5), (8) and (9) and mean diameter and average support densities.
[d] Derived from Fig. 3b.
[e] Manufacturer's specifications.

m^{-3} for agarose and steel, respectively, it was found that the density approached 6640 kg m^{-3} for certain adsorbent particles (see, for example, Fig. 2b), i.e., those encased in a very thin agarose layer, whereas large adsorbents containing small cores possessed densities of less than 3000 kg m^{-3} in some cases (Fig. 2c). The average density of the prototype adsorbents was measured to be between 3960 and 4780 kg m^{-3} (Table 1). Although the ratios between largest and smallest diameter of each prototype were less than 2.2 (except for p-4), the wide distribution of densities leads to ratios of the minimum fluidisation velocities greater than 2, indicating that the supports can be expected to form a classified fluidised bed when expanded [4]. The different size and density distributions of the prototypes reflect that they were produced from different batches of underivatised supports. For the commercial materials, densities similar to those provided by the manufacturer were recorded.

4.2. Bed expansion

The theoretical fluidisation properties of the supports were determined using Eqs. (1), (2)–(5) and (8)–(9) and are listed in Table 1. The U_t values for each batch were predicted using Eq. (1) and the Re_t for the prototypes were between 0.069 and 0.083, resulting in n-index values of ~4.72. The Re_{mf} values were 0.001 (Table 1) suggesting that superficial fluid velocities greater than ~12 cm h^{-1} were necessary for fluidisation of these materials. The expected bed heights and folds of expansion for the p-2, U-1 and S-1 matrices were determined using Eqs. (6) and (7) and gave the series of lines shown in Fig. 3a. The experimentally determined data for expansion of both the prototype and commercial adsorbents are also presented in Fig. 3a.

The observed expansion of the prototype matrices was ~1.5–3-fold at superficial fluid velocities between ~50 and 250 cm h^{-1} (Fig. 3a). There were only small differences between the prototypes, however the results indicate that expansion followed the order: p-2 > p-4 = p-1 > p-3. Although this may suggest that the variation in size and density distributions had a small effect on the fluidisation properties, it is difficult to draw any correlation with the physical characteristics presented in Table 1. Fur-

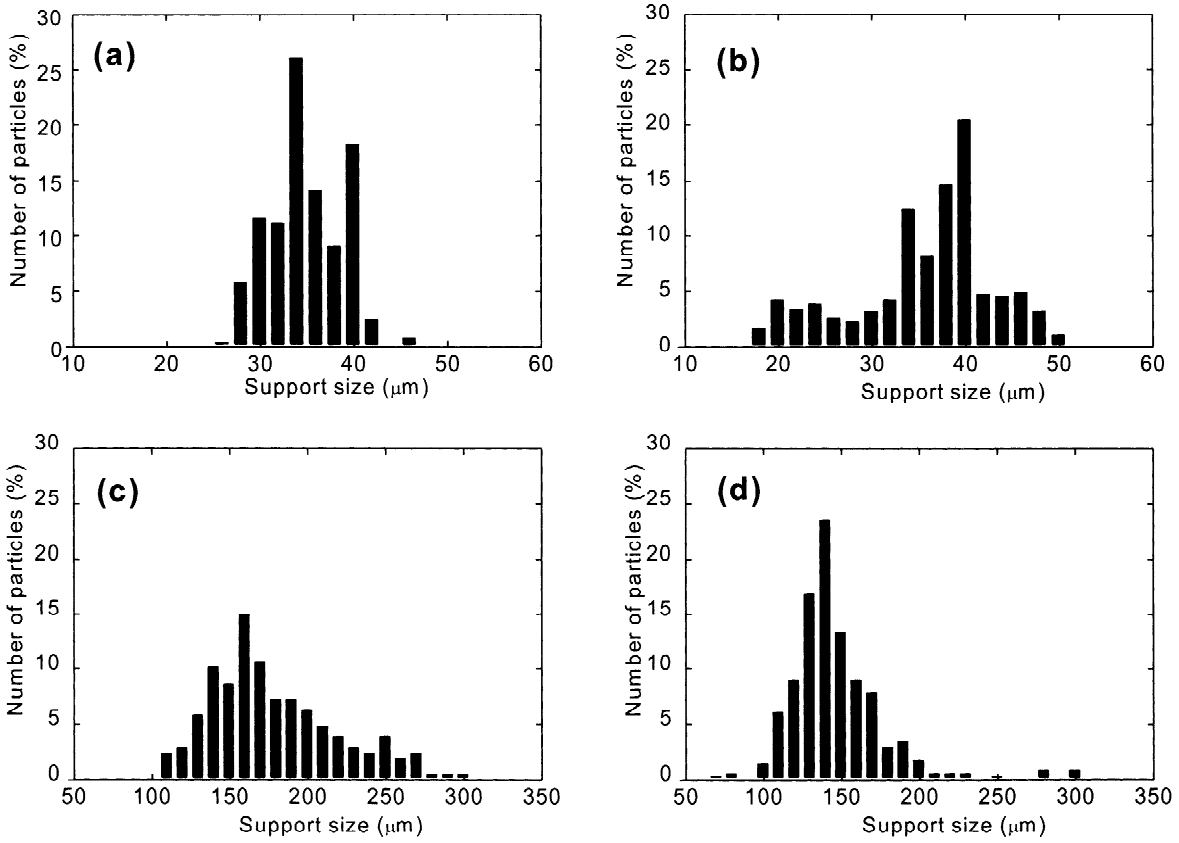

Fig. 1. Support size distribution profiles for: (a) p-2; (b) p-4; (c) U-2; (d) S-1. In each case between 260 and 460 particles were counted.

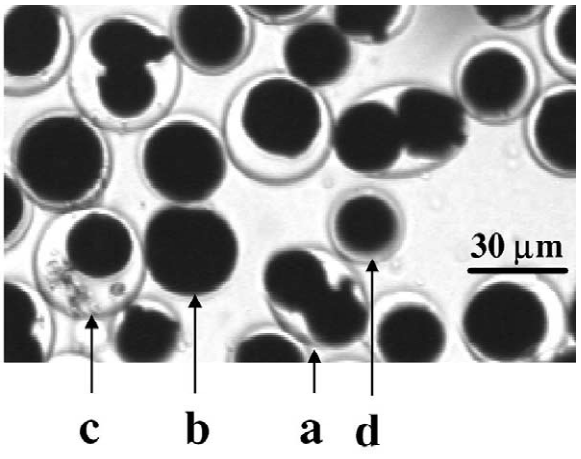

Fig. 2. Light micrograph of the p-2 support at ×20 magnification: (a) Bi-cored support, (b) large single-cored support with ultra-thin agarose layer, (c) large support with thick agarose layer and small core, (d) small support with thin agarose layer. Approximate densities are (kg m^{-3}): 3410, 6640, 2280 and 4000 for a, b, c and d, respectively.

thermore, although the supports were variously derivatised, a specific study using the same original batch of particles would be required to conclude what role the ligands play in fluidisation behaviour. The Richardson–Zaki correlation predicted lower expansion for the prototypes than that which was observed, whereas for the STREAMLINE supports the reverse was seen (Fig. 3a). The closest fit of theoretical to experimental data was obtained with the UFC supports.

In light of the discrepancy between the model and experimentally obtained expansion curves, the data from Fig. 3a were replotted (Fig. 3b) to calculate the values of the expansion index n and U_t for each support. From the results presented in Table 1, it is apparent that for all the prototypes, the experimentally determined n-index value (5.02–5.81) was higher than that predicted (4.72) using Eq. (3) and that the values for the prototype adsorbents were slightly lower than those for the 100–300 μm commercial

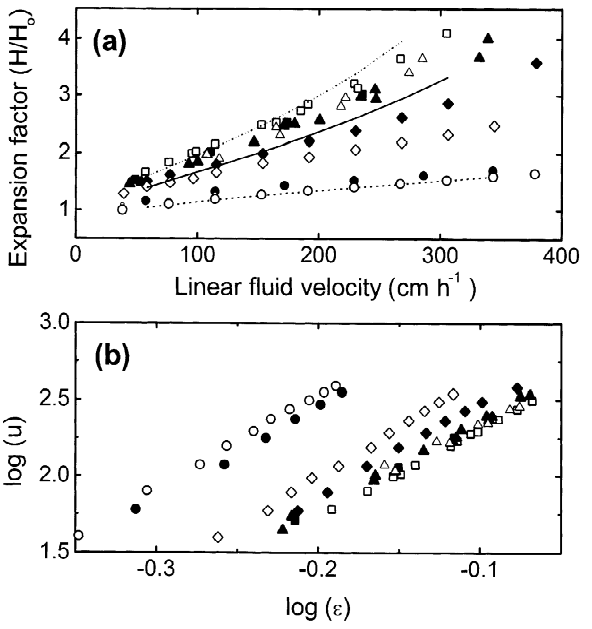

Fig. 3. (a) Comparison of data for bed expansion versus superficial linear fluid velocity determined using the Richardson–Zaki correlation (lines) and experimentally obtained (symbols). Prototype matrices: (■) p-1, H_o=6 cm; (□, —) p-2, H_o=5.25 cm; (▲) p-3, H_o=6.1 cm; (△) p-4, H_o=5.5 cm. Commercial matrices: (●, - - -) U-1, H_o=6.6 cm; (○) U-2, H_o=5.2 cm; (♦, – .. – .. –) S-1, H_o=5.45 cm; (◇) S-2, H_o=5.6 cm. (b) Experimental expansion data from (a) re-plotted to allow determination of slope (*n*-index) and *y* intercept (U_t); same symbols apply as those used in (a).

supports (6.10–6.55). Despite the fact that the prototype supports expand to a greater extent than the commercial ones due to a lower U_t, their lower *n* value indicates that they expand proportionately less as flow-rate is increased than the commercial materials. The experimentally determined U_t and Re_t of the prototype adsorbents were within 12% of the theoretical values (Table 1). However, the experimentally determined U_t values for the commercial supports were much higher than those predicted from Eq. (1), but were within the range expected from the minimum and maximum support diameters.

The above results indicate that the Richardson–Zaki correlation does not adequately forecast the fluidisation behaviour of the EBA matrices in the experimental system used in this work. A number of other workers have also reported values for the expansion index *n* for EBA supports which vary from that predicted by the Richardson–Zaki correlation [5,8,27,28]. For example, Karau et al. [5] found that the experimentally determined *n* value increased from 4.9 to 5.5 as the size of DEAE-linked supports was reduced from 250–300 to 120–160 μm. Furthermore, the calculated U_t for the 120–160 μm adsorbent was much higher (1326 cm h^{-1}) than that obtained experimentally (654 cm h^{-1}). The authors speculated on support agglomeration as the cause for these disparities. In the current work, agglomeration was not observed and it is difficult to determine the precise reason for the discrepancy between the predicted and observed bed expansion. However, it is likely that a number of factors act in concert and three possibilities have been identified: (i) support size and density distribution; (ii) support shape and (iii) the method of fluid distribution.

The differences in density of particles within the same batch of prototypes, combined with an asymmetric size distribution (see Fig. 1), could lead to skewing of the terminal settling velocities in the support population. As flow-rate was increased, a bed with a support population having larger numbers of small or less dense particles (Figs. 1b and 2) would expand more than expected from measurements of average size and density and the assumption of a bell-shaped distribution, and would therefore give a higher *n* value than predicted.

Finette et al. [8] found that the non-spherical shape of EBA supports (40–63 μm diameter particles) resulted in a higher experimentally determined *n*-index (5.28) than that predicted using the Richardson–Zaki correlation (4.8). These workers also reported deviations of 20–50% between the theoretical and experimentally derived U_t values. In the current work, between 8 and 46% of the prototype support population had more than one core particle, leading to non-spherical (typically ellipsoid) shapes. In all cases the observed value of *n* was higher than that predicted from the Richardson–Zaki correlation (Table 1) which is consistent with the results of Finette et al. [8] and also with the conclusion of Di Felice [29] that the experimentally determined value of *n* is always greater for irregular particles than that for spheres. A direct quantitative relation to the shape factor is still lacking [29].

The importance of a plate in ensuring even fluid distribution is well known, but according to Di

Felice [29] the effect of the distributor on bed expansion and fluidisation quality has never been systematically studied. The EBA column employed in the experiments presented here uses a localised stirring zone to distribute fluid [18]. Turbulence from the distributor could be expected to cause deviations from plug flow leading to channeling and fluid jet streams which may reduce expansion. Conversely, the stirring used could lead to increased voidage in the column bottom. The bed would therefore expand to a greater extent than predicted from the Richardson–Zaki correlation, as was observed (Fig. 3a). Evidence for a complex effect on fluidisation of the distributor was seen in the current work when expansion curves with different bed heights were conducted in 0.1 *M* Tris–HCl buffer, pH 7. It was observed that increasing the settled bed height from 6.3 to 10 cm exerted little impact on the expansion curve of support p-1 ($U_t = 646$ and 653 cm h^{-1}, and $n = 5.03$ and 5.2, respectively). However, lowering the settled bed height to 3.7 cm, markedly reduced the degree of expansion, consistent with poor fluid distribution and channeling, and U_t rose to 805 cm h^{-1}. Furthermore, the value for n rose to 5.4, which would normally be consistent with better fluid flow through the bed. In this case it may reflect an increase in turbulence, causing the bed to expand proportionately more would be expected. The finding that a higher settled bed resulted in better expansion of the support can be explained by a suggestion put forward by De Luca et al. [28]. The lower part of the bed is believed to act as a fluid distributor which also dampens turbulence and any channeling caused by the actual distributor. Therefore, with a higher amount of settled adsorbent, the proportion of the bed experiencing good fluid flow increases.

The STREAMLINE supports expanded much less than expected based on theoretical calculations using the measured size and density (Fig. 3a), although the experimental U_t values (1221 and 2005 cm h^{-1} for S-1 and S-2, respectively) were similar to those reported by other workers using STREAMLINE adsorbents (between ~600 and ~1600 cm h^{-1}; see, for example, Refs. [5,6,28,30]).

In biotechnology, values of n and U_t predicted by the Richardson–Zaki correlation are widely quoted (see, for example, Refs. [1,2,6,8,27]) even though many workers subsequently use experimental data to find n and U_t for the combination of support, column and feedstock to be used. Taken together with the above discussion, this implies that there is a lack of validity inherent in the assumptions made in using the Richardson–Zaki correlation for the setup used in this work and for EBA generally. According to Al-Dibouni and Garside [3], the average characteristic approach cannot be used for ratios of smallest to largest particle greater than 1.3 given that stratification occurs during fluidisation. Furthermore, there is a balance between the mixing effects attributable to axial dispersion and the segregating effect of the particles [4]. Further work to examine, validate and eventually extend alternative models such as the ''beds-in-series'' approach [2,3,31] for EBA systems using supports of varying shape and columns with non-ideal fluid distributors should be pursued.

4.3. Residence time distribution studies

The fluidisation studies showed that the distributor had an effect on expansion of the matrix, particularly at settled bed heights below 6 cm; however, the implication of the stirring on the amount of axial dispersion in the column was unclear. RTD studies were therefore undertaken to determine whether the numbers of theoretical plates developed by small amounts of the support (~6 cm settled bed) were sufficient for a small-scale EBA process applicable to rapid screening purposes. The residence time distribution of a negative step input of acetone tracer was used to calculate D_{axl} using Eq. (12), given that the vessel dispersion numbers were in all cases greater than or equal to 0.01 [20].

Fig. 4a shows the effect of increasing interstitial fluid velocity on axial dispersion within expanded beds of prototype adsorbents. For all supports tested, a clear tendency for D_{axl} to rise in response to increases in U_i was observed. The trend was essentially proportional, except for support p-1. Apparently conflicting information was obtained from plots of N (Fig. 4b) against superficial linear fluid velocity. N was seen to increase gradually, reaching >40 plates at a linear fluid velocity of 340 cm h^{-1}, suggesting that overall column performance was improved at the highest fluid velocities. However HETP increased for all supports over the same range of flow-rates

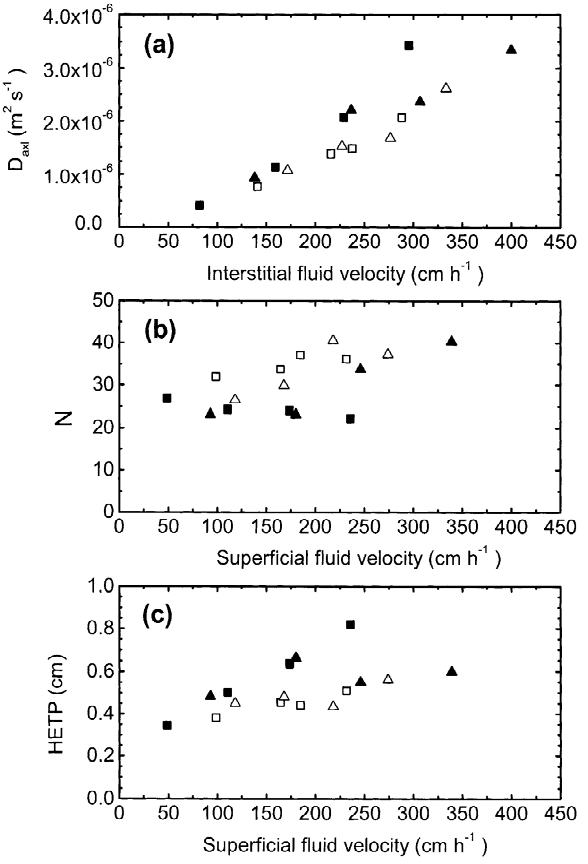

Fig. 4. Hydrodynamic properties of the prototype supports. Relationship between: (a) coefficient of axial dispersion and interstitial fluid velocity; (b) number of theoretical plates and superficial fluid velocity and (c) HETP and superficial fluid velocity. Symbols: (■) p-1, H_o=6 cm; (□) p-2, H_o=5.9 cm; (▲) p-3, H_o=6.1 cm; (△) p-4, H_o=6.2 cm.

suggesting that ''packing quality'' was affected in the bed (Fig. 4c).

A very recent study by Pålsson et al. [14] comparing dispersion in packed and expanded beds revealed similar contradictions to those observed in this work. The authors concluded that the quantities *N*, HETP and Bodenstein number (i.e., reciprocal of the vessel dispersion number), send out misleading information when applied to expanded beds. They argued that the conventional approach of using bed height and residence time as a measure of the separation distance is not consistent with the operation of expanded beds, where the void fraction is strongly dependent on the fluid velocity applied. Moreover, given that separation can only occur when species interact with matrix particles and not within the surrounding liquid Pålsson et al. [14] argued that it was incorrect to assign plates arising from the void between particles to the matrix. In view of this, Pålsson et al. [14] introduced the parameters $HETP_{EB}$ and N_{EB}, which relate HETP and *N* to the settled bed height according to Eqs. (14) and (15):

$$N_{EB} = (H_o/\sigma_H)^2 = (H/\sigma_H)^2/(H/H_o)^2 = N/(H/H_o)^2 \quad (14)$$

$$HETP_{EB} = H_o/N_{EB} = HETP \cdot (H/H_o) \quad (15)$$

where σ_H is the standard deviation of the tracer in units of column length.

Factors affecting axial mixing in EBA are still not well understood [26]; however, it is known that protein adsorption in EBA columns is governed by diffusive effects (pore and film mass transfer) as long as the flow through the bed is of sufficient quality, i.e., axial dispersion is low, and the mean residence time of fluid in the bed is long. A more conventional description of an EBA column is that the total number of theoretical plates (Fig. 4b), which is proportional to the value of the vessel dispersion number (Eqs. (10)–(13)) measured using a rapidly diffusing tracer such as acetone, reflects the mixing in the total column set-up of fluid and resin where the protein separation is to take place. Plate number is a function of dispersed flow (D_{axl}) and convective flow ($U \cdot H/\varepsilon$) [21] and increases in *N* can occur as *U* is raised if the dispersive contribution does not rise proportionately to the convective flow. In the current work, the results for D_{axl} (Fig. 4a) and *N* (Fig. 4b) for supports p-2, p-3 and p-4 suggest that as fluid velocity is raised, D_{axl} increases; however, the overall mixing in the complete column is reduced due to the longer bed length. For support p-1 however, plate number decreases because D_{axl} increases disproportionately to increases in U_i (Fig. 4a). In contrast to the effect of *U* on HETP observed here, Yamamoto et al. [26] found that for EBA columns with STREAMLINE matrices, HETP was between 0.8 and 1.5 cm and did not significantly depend on the flow-rate (2 to ~10 cm min^{-1}), settled bed height (4.2–9.1 cm) or column diameter (1.6–2.6 cm). This difference in the trend for HETP likely

reflects the use of less turbulent fluid distribution in the work of Yamamoto et al. [26] than in the current work.

Previous workers have shown that a successful EBA process typically requires ~30 theoretical plates [2,19] and the results presented here (Table 2) indicate that the small amounts of support used gave properties suitable for EBA. Table 2 collates dispersion data from the current study together with values reported by other workers using different expanded bed support materials. Similar fluid velocities (i.e., 233–300 cm h^{-1}) were chosen for this comparison. The small stainless steel cored pellicular supports described in the current work possess hydrodynamic properties similar to those reported by Pålsson et al. [13,14] for materials of like construction, but bigger size, and are superior to all of the other adsorbents listed (STREAMLINE, fluoromodified zirconia and UFC). The HETP values determined for the small steel-cored prototypes in this work were however 2–3-fold higher than those reported by Pålsson et al. [14] for a 32–75 μm steel–agarose composite of similar density. This is most probably related to the higher D_{axl} values ($2–3.4\times10^{-6}$ compared to 1.6×10^{-6}), which arise from the combination of a localised stirring fluid distribution system used in the current work and the higher degree of bed expansion (~3-fold compared to 2-fold) of the smaller matrix particles.

5. Conclusions

The Richardson–Zaki correlation is unsuitable for

Table 2
Comparison of dispersion data for the prototype adsorbents with other expanded bed supports

Support			Column diameter and distributor[a]	Tracer	H_o (cm)	H (cm)	U (cm h^{-1})	D_{axl} ($\times10^{-6}$ m^2 s^{-1})	Reciprocal of vessel dispersion number	N	HETP (cm)	Refs.
Type	d_p (μm)	ρ_p (kg m^{-3})										
p-1	28–44	3960	1 cm LS	Acetone	6	17.9	237	3.4	43	32	0.81	This work
p-2	26–46	4330	1 cm LS	Acetone	5.9	18.1	233	2.0	71	36	0.50	This work
p-3	26–42	4780	1 cm LS	Acetone	6.1	18.5	246	2.36	66	34	0.55	This work
p-4	18–50	4250	1 cm LS	Acetone	6.2	20.9	274	2.62	74	37	0.56	This work
Steel/agarose	32–75	4400	1 cm sintered plastic filter	BSA	6.1	12.2	248	1.6	76	38	0.32	[14]
STREAMLINE prot.A	80–165	1300	1 cm sintered plastic filter	BSA	5.9	11.8	264	3.1	37	18	0.64	[14]
STREAMLINE DEAE	100–300	na	2.5 cm plate and mesh	Acetone	15	42	300	na	na	50–70	0.84–0.6	[19]
STREAMLINE DEAE	100–300	na	60 cm plate and mesh	Acetone	15	45	300	na	na	35–50	1.3–0.9	[19]
zirconia	38–75	2800	2.5 cm plate and mesh	Sodium nitrite	9.3	18.6	257	na	17	8.5[b]	2.2[b]	[32]
STREAMLINE SP	100–300	1184	5 cm plate and mesh	Acetone	10	20	300	6.35	37	19	1.05	[30]
STREAMLINE SP XL	100–300	1300	2.5 cm plate and mesh	Acetone	15.3	39	300	88.3	36.4	18.7	2.11	[25]
UFC DEAE	100–300	1300–1500	2 cm LS	Acetone	22	44	300	na	na	45	1.0	[18]

LS, localised stirring fluid distributor; na, not available.

[a] Studies conducted with water except for: 100 m*M* phosphate [14]; 50 m*M* Tris–HCl [19]; 50 m*M* MES 100 m*M* NaF [32]; and 100 m*M* acetate [30].

[b] Calculated assuming: reciprocal of vessel dispersion number = 2*N* (see Eqs. (10)–(13)).

predicting the fluidisation behaviour of the experimental set-up used in this work and for EBA in general, given that the assumptions regarding support and column properties are not valid. Reducing the diameter of support particles to a range between 18 and 50 μm while increasing the density using a stainless steel core material, results in EBA adsorbents with hydrodynamic properties that are significantly enhanced compared with much larger commercially available materials. Future work should now be undertaken to establish whether the enhanced features of the prototype expanded bed adsorbents described in this work can be exploited advantageously in complex particulate containing systems.

6. Nomenclature

d_c	column diameter (m)
d_p	particle diameter (m)
D_{axl}	liquid axial dispersion coefficient ($m^2\ s^{-1}$)
g	acceleration due to gravity ($m\ s^{-2}$)
Ga	Gallileo number
H	height of expanded bed (m)
HETP	height equivalent to a theoretical plate (cm)
H_o	height of settled bed (m)
n	Richardson-Zaki expansion index
N	number of theoretical plates
Re_{mf}	particle Reynolds number at minimum fluidisation
Re_p	particle Reynolds number
Re_t	particle Reynolds number at terminal settling velocity
t_m	mean residence time of tracer (s)
U	superficial fluid velocity ($m\ s^{-1}$)
U_i	interstitial fluid velocity ($m\ s^{-1}$)
U_{mf}	minimum fluidisation velocity ($m\ s^{-1}$)
U_t	terminal settling velocity of a particle ($m\ s^{-1}$)
ε	expanded bed voidage
ε_o	settled bed voidage
η	solution viscosity ($kg\ m^{-1}\ s^{-1}$)
ρ_p	particle density ($kg\ m^{-3}$)
ρ_l	liquid density ($kg\ m^{-3}$)
σ	standard deviation of tracer residence time (s)
σ^2	variance of tracer residence time (s^2)
σ_H	standard deviation of tracer in the units of column length (m)
$\sigma_\theta{}^2$	dimensionless variance of tracer

Acknowledgements

We thank the Danish Technical Research Council (Statens Teknisk Videnskabelige Forskningråd) for funding this work and Irini Theodossiou gratefully acknowledges financial support from a Marie Curie Research Training Grant (No. ERB4001GT972611) and the Center for Process Biotechnology, BioCentrum-DTU. Finally the authors wish to thank Up-Front Chromatography A/S for manufacturing the prototype supports and Niels Mathiasen for technical assistance.

References

[1] N.M. Draeger, H.A. Chase, Trans. IChemE 69 (1991) 45.
[2] R. Hjorth, P. Leijon, A.K. Barnfield Frej, C. Jägersten, in: G. Subramanian (Ed.), Bioseparation and Bioprocessing, Vol. 1, Wiley, Weinheim, 1998, p. 199, Chapter 9.
[3] M.R. Al-Dibouni, J. Garside, Trans. IChemE 57 (1979) 94.
[4] J.M. Coulson, J.F. Richardson, J.R. Backhurst, J.H. Harker, in: Chemical Engineering, 4th ed., Vol. 2, Pergamon, Oxford, 1991.
[5] A. Karau, C. Benken, J. Thömmes, M.-R. Kula, Biotechnol. Bioeng. 55 (1997) 54.
[6] J. Thömmes, Adv. Biochem. Eng. Biotechnol. 58 (1997) 183.
[7] W.T. Tang, L.S. Fan, Chem. Eng. Sci. 45 (1990) 543.
[8] G.M.S. Finette, Q.M. Mao, M.T. W Hearn, J. Chromatogr. A 743 (1996) 57.
[9] M.A. Olander, T. Mollegaard, A. Lihme, I. Theodossiou, T.J. Hobley, O.R.T. Thomas, in: Abstracts of the 4th International Conference on Separations for Biotechnology, March 1999, Reading, UK, p. 7.
[10] M.A. Olander, A.O.F. Lihme, T.J. Hobley, M. Simón, I. Theodossiou, O.R.T Thomas, PCT WO 00/57982 (2000).
[11] I. Theodossiou, M.A. Olander, M. Søndergaard, O.R.T. Thomas, Biotechnol. Lett. 22 (2000) 1929.
[12] I. Theodossiou, M. Søndergaard, O.R.T. Thomas, Bioseparation 10 (2001) 31.
[13] E. Pålsson, P.-E. Gustavsson, P.-O. Larsson, J. Chromatogr. A 878 (2000) 17.

[14] E. Pålsson, A. Axelsson, P.-O. Larsson, J. Chromatogr. A 912 (2001) 235.
[15] A. Lyddiatt, D. O'Sullivan, Curr. Opin. Biotechnol. 9 (1998) 177.
[16] J. Thömmes, A. Bader, M. Halfar, A. Karau, M.-R. Kula, J. Chromatogr. A 752 (1996) 111.
[17] J.F. Richardson, W.N. Zaki, Trans. IChemE 32 (1954) 35.
[18] E. Zafirakos, A. Lihme, Bioseparation 8 (1999) 85.
[19] A.K. Barnfield Frej, H. J Johansson, S. Johansson, P. Leijon, Bioprocess Eng. 16 (1997) 57.
[20] O. Levenspiel, in: Chemical Reaction Engineering, 3rd ed., Wiley, New York, 1999.
[21] F.B. Anspach, D. Curbelo, R. Hartmann, G. Garke, W.D. Deckwer, J. Chromatogr. A 865 (1999) 129.
[22] J.M. Kay, R.M. Nedderman, in: Fluid Mechanics and Transfer Processes, Cambridge University Press, Cambridge, 1985.
[23] D. Kunii, O. Levenspiel, in: Fluidization Engineering, 2nd ed., Butterworth-Heinemann, Stoneham, 1991.
[24] O. Levenspiel, in: Chemical Reaction Engineering, 2nd ed., Wiley, New York, 1972.
[25] N. Ameskamp, C. Priesner, J. Lehmann, D. Lütkemeyer, Bioseparation 8 (1999) 169.
[26] S. Yamamoto, N. Akazaki, O. Kaltenbrunner, P. Walter, Bioseparation 8 (1999) 33.
[27] C.M. Griffith, J. Morris, M. Robichaud, M.J. Annen, A.V. McCormick, M.C. Flickinger, J. Chromatogr. A 776 (1997) 179.
[28] L. DeLuca, D. Hellenbroich, N.J. Titchener-Hooker, H.A. Chase, Bioseparation 4 (1994) 311.
[29] R. Di Felice, Chem. Eng. Sci. 50 (1995) 1213.
[30] Y.K. Chang, H.A. Chase, Biotechnol. Bioeng. 49 (1996) 512.
[31] N. Epstein, B.P. Leclair, B.B. Pruden, Chem. Eng. Sci. 36 (1981) 1803.
[32] A. Mullick, M. Flickinger, Biotechnol. Bioeng. 65 (1999) 282.